Real-Time Weld Quality Prediction in Automated Stud Welding: A Data-Driven Approach

Beatriz Coutinho[1][a], Bruno Santos[1][b], Rita Gomes Mendes[2][c], Gil Gonçalves[1][d] and Vítor H. Pinto[1][e]
[1] *SYSTEC ARISE, Faculdade de Engenharia, Universidade do Porto, Rua Dr. Roberto Frias, 4200-465 Porto, Portugal*
[2] *ISQ&CTAG Automotive Technologies, Monção, Portugal*

Keywords: Stud Welding, Weld Quality Prediction, Sensorisation, Data Acquisition.

Abstract: Drawn arc stud welding is extensively used in automotive assembly lines for attaching components to vehicle bodies. In these automated processes, low-quality welds can compromise structural integrity and cause production delays due to rework and maintenance. This paper describes the initial development stage of an artificial intelligence (AI)-based system for real-time weld quality prediction in automated stud welding. The focus of this first phase is on implementing sensorisation, developing a data acquisition system, and constructing a dataset that captures the most relevant process variables characterizing the welding process. A Flask-based application was developed to facilitate data collection, incorporating an automatic character recognition algorithm to extract parameters directly from the control unit display. Initial welding experiments produced a dataset of approximately 200 samples, with preliminary data analysis validating expected parameter trends. The results confirm the system's capability to effectively capture relevant data, forming the basis for future development of a predictive model aimed at enhancing weld quality monitoring and minimizing assembly line interruptions.

1 INTRODUCTION

Drawn arc stud welding (SW) is a process that uses an electric arc to fuse a metal stud to a workpiece. It is widely used across various manufacturing sectors due to its fast cycle time, and the simplicity and cost-effectiveness of the equipment involved (Klaric et al., 2010). The SW process involves generating an electric arc between the stud and the workpiece (Figure 1b), which melts both the surface of the workpiece and the tip of the stud. Once the materials are molten, the stud is pressed into the workpiece (Figure 1c), and as the metal cools and solidifies, it forms a strong and permanent bond (Figure 1d) (T. Lienert, 2011).

In the automotive industry, SW is commonly used on assembly lines to attach different components to the car body, with the process typically being fully automated. Low-quality welds in these automated lines can have a significant impact. If undetected, they may compromise the structural integrity of the final product, and even when detected, they lead to frequent interruptions for maintenance and manual rework, reducing overall efficiency and causing production delays.

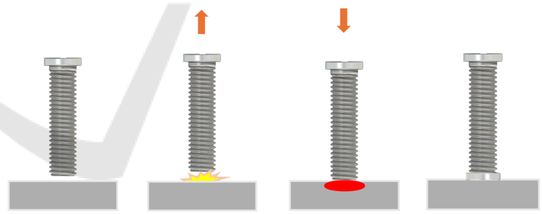

(a) Stud positioning. (b) Lift. (c) Plunge. (d) Welded stud.

Figure 1: Arc stud welding process.

This work addresses this issue by proposing the development of an artificial intelligence (AI) model capable of predicting, in real-time, if a weld will be defective. To achieve this, two main stages are re-

[a] https://orcid.org/0009-0000-9769-6726
[b] https://orcid.org/0009-0007-6038-6506
[c] https://orcid.org/0009-0008-9899-6729
[d] https://orcid.org/0000-0001-7757-7308
[e] https://orcid.org/0000-0002-7840-0333

Coutinho, B., Santos, B., Mendes, R. G., Gonçalves, G. and Pinto, V. H.
Real-Time Weld Quality Prediction in Automated Stud Welding: A Data-Driven Approach.
DOI: 10.5220/0013714100003982

In *Proceedings of the 22nd International Conference on Informatics in Control, Automation and Robotics (ICINCO 2025) - Volume 1*, pages 251-258
ISBN: 978-989-758-770-2; ISSN: 2184-2809

quired: (1) the construction of a dataset containing key process variables that reflect weld quality, and (2) the selection, training, and testing of a supervised machine learning (ML) algorithm to predict the weld quality outcomes. This project is part of the *GreenAuto Agenda*, co-financed by the Portuguese Recovery and Resilience Plan, that aims to position the national automotive industry within the value chain of low-emission vehicles (Agenda GreenAuto, 2021).

This paper primarily focuses on the first development stage: the construction of the dataset . Section 2 presents a literature review supporting the selection of relevant process parameters. Section 3 outlines the methodology, including the welding environment setup, welding experiments, and the key parameters identified for assessing weld quality. Section 4 focuses on the implementation details of the sensorisation setup and the data acquisition system and methods. Section 5 presents the implementation results along with a preliminary data analysis. Lastly, Section 6 summarizes the main findings and future work directions.

2 LITERATURE REVIEW

Accurately estimating and predicting the quality of the stud weld requires identifying the most relevant process parameters and selecting the appropriate analysis methods. This Section reviews studies on SW to help determine the key parameters that best characterize the process.

In (Naddaf-Sh et al., 2023), an AI-based approach was proposed to detect and classify defects in SW. An experimental setup was created to intentionally produce defective welds while recording parameters such as voltage, welding current, linear motor current, and pin displacement. The study concluded that welding voltage and pin lift distance were the most influential factors in defect classification.

Similarly, (Samardzic et al., 2007) explored the effects of welding voltage and current on weld quality by applying the process to surfaces with varying contamination levels, such as dust and rust, while keeping other variables constant. The findings reiterated that welding voltage plays a critical role in identifying defects, however changes in current alone were found to be insufficient.

In (Klaric et al., 2010), several factors, such as welding current, process duration, and stud plunge and lift were evaluated to assess their impact on weld penetration depth. The analysis revealed that welding current and duration were the most significant factors.

Another author (Chambers, 2001) examined the fundamental principles of SW to support better interpretation of results. It emphasized the importance of parameters like pin motion, process duration, and current, as well as the condition of the welding equipment and environment. Factors such as dust, humidity, and high machine temperatures were found to degrade components, especially electrical cables, consequently affecting weld quality. The study also highlighted more process specific parameters, including the pin immersion depth, lift distance, weld duration, current, and pin-to-plate alignment, as valuable for characterizing the process.

Lastly, (Al-Sahib et al., 2009) emphasized the significance of electrical parameters, particularly current, in assessing weld quality. The analysed metrics included root mean square (RMS), average, time-integrated, and peak current, identifying peak current as the most indicative of weld quality. It also discussed how the welding duration, current range, plate thickness, and pin diameter affect the process. Additionally, the study highlighted challenges in using external sensors due to heat, splatter, fumes, and electromagnetic noise generated during welding.

3 METHODOLOGY

The SW process being modelled involves the attachment of metal studs to metal plates, as seen in Figure 2, as part of an automotive assembly line. The process is carried out using an LM310 welding head, which is powered by a DCE1500 control and energy unit.

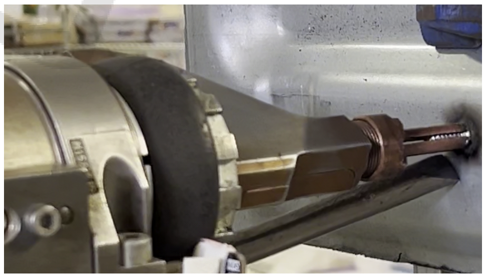

Figure 2: Stud welding process.

The DCE1500 unit features a small display that shows some process parameters measured by the system itself after each weld, such as the arc voltage in the pilot current phase, arc voltage in weld current phase, weld current, welding process duration, stud drop time, lift distance and process energy, as illustrated in Figure 3. Figure 4 outlines the typical welding cycle under DCE1500 control, showing the temporal evolution of arc voltage, welding current, and stud movement.

(a) DCE1500 control unit display.

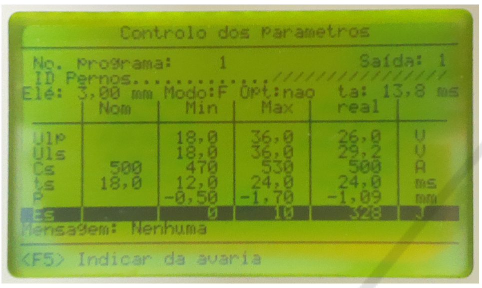

(b) Displayed process parameters (close-up).

Figure 3: Welding system control and display panel.

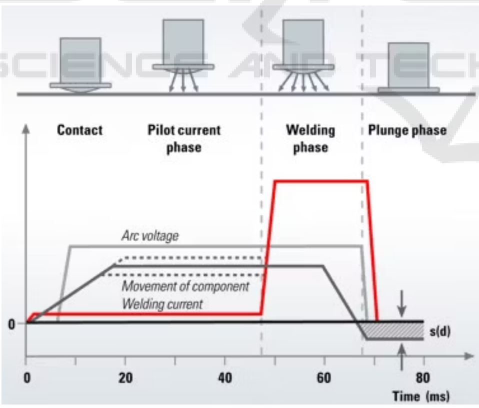

Figure 4: Typical stud welding cycle under DCE1500 control (PT. Unggul Semesta,).

Since the objective is to run the predictive model in real-time during production, a Physical Twin of the welding system was developed to enable model development and testing in a non-disruptive way. This Physical Twin will be used in the early project stages to collect data and perform welding experiments, before the deployment on the assembly line.

The literature review presented in Section 2 guided the selection of the variables to be monitored in this case study. These studies helped anticipate how different welding parameters can affect the final weld quality and revealed potential challenges in modelling the SW process. As a result, the variables listed in Table 1 were considered to be monitored for their potential to accurately characterize the SW process, and therefore support the successful development of the weld quality prediction model.

4 IMPLEMENTATION

This Section details the implementation of the developed system.

4.1 Sensorisation

Among the parameters listed in Table 1, electrical quantities such as voltage and current stand out as essential for assessing the quality of the SW process. The temperature reached by the plate during the welding is also a critical factor, as inadequate values can result in excessive or insufficient fusion of the components, jeopardising the final weld quality. Other important parameters include the distance between the welding gun and the plate, as well as the inclination of the plate during the process. Environmental conditions, specifically the concentration of carbon monoxide (CO), ambient humidity, and temperature, were also considered essential to monitor due to their potential influence on process stability.

Considering this, the following sensors were selected:

- **LEM HTFS 800-P:** a current sensor, capable of measuring currents until 1200A with an accuracy of 1%. Utilised to measure the welding process current.
- **MLX90614-DCI:** an I2C non-contact infrared (IR) temperature sensor, suitable for industrial applications due to its small field of view (FOV) of 5º. It is capable of measuring temperatures between -70ºC and 270ºC with an accuracy of 0.5ºC. Utilised for measuring the plate temperature.
- **MQ-7:** a CO sensor, capable of detecting CO concentrations in the air from 20 to 2000 parts per million (ppm). Utilised to measure the air quality during the welding process.
- **BME688:** an I2C environmental, utilised for measuring the ambient temperature and humidity. It is capable of measuring temperature between 0ºC and 65ºC with an accuracy of 0.5ºC and rel-

Table 1: Relevant parameters to monitor during the welding process.

Category	Variables
Electric Quantities	Voltage, Current (peak, effective, and average), Power
Process Parameters	Stud lift distance, Stud immersion length, Stud incidence angle, Process time duration
Environmental Parameters	Ambient temperature, Ambient humidity, Air purity
Other Factors	Temperature of materials (stud and plate), Temperature of machinery (head and feeder), Cleanliness of the equipment (head, stud, and plate), Current/Speed of the linear actuator, Cooling rate of welding
Discarded Factors	Factors dependent on the materials of the studs and plates (composition, purity, dimensions, etc.)

ative humidity (RH) between 20% and 80% with an accuracy of 3%.

- **LM35:** a temperature sensor, capable of measuring temperatures between 0ºC and 100ºC. Utilised to measure the ambient temperature during the welding.
- **VL53L0X:** a time-of-flight (ToF) high-precision distance sensor, capable of measuring distances between 30mm and 2000mm with an accuracy of 3%. Utilised for measuring the plate distance.
- **YDLIDAR GS2**: a linear array solid Light Detection and Ranging (LiDAR) sensor with a FoV of 100º capable of measuring distance in a range between 25mm and 300mm with an accuracy of 8% for distances superior than 200mm. Utilised to measure the plate inclination angle, corresponding to the stud incidence angle.

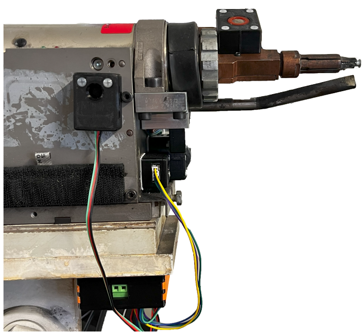

Figure 5: Welding system sensorisation.

Figure 5 illustrates the installation of sensors in the Factory Twin. The CO sensor is mounted on the top, the temperature sensor on the side, and the distance and plate inclination sensors are positioned at the front. The sensors not visible in the image, such as the humidity sensor and the current sensor attached to the welding system's ground cable, are installed on the opposite side.

To acquire the data from the sensors, two Arduino Nano boards were used: one exclusively dedicated to capturing high-frequency data from the current sensor, and the other for the remaining sensors.

4.2 Data Acquisition System

To store the collected data in an organized and structured manner, a data acquisition system was developed. The two previously mentioned Arduino Nano boards were connected to a Raspberry Pi 5 (RPI5), running a Flask-based data acquisition application developed using Python, HTML, JavaScript, and CSS. Because the parameters measured and displayed by the welding system itself could not be directly accessed, but were still considered relevant, the RPI5 was also connected to a camera to capture images of the values shown on the DCE1500 display. Additionally, a RPI touch display was used to provide a graphical user interface (GUI).

The GUI, illustrated in Figure 6, allows users to start and stop the sensor data recording at appropriate moments during the welding tests, while tracking the weld identifiers (IDs) to maintain organized records. During recording, real-time values from the Arduino boards and the camera are displayed, allowing users to confirm that the data is being captured as expected. After recording, the user should capture an image of the DCE1500 display using the system. Once both sensor data and the image are collected, they are automatically saved: the sensor data as a comma-separated values (CSV) file and the image as

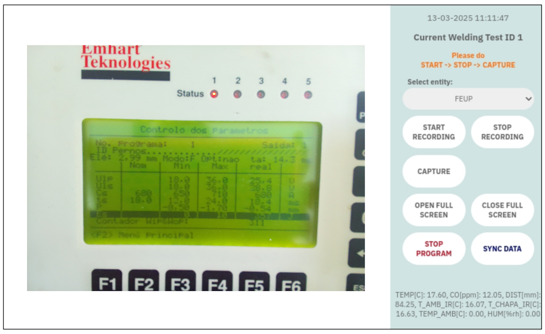

Figure 6: Data acquisition application GUI.

a separate file. Both files are named using the recording date and the corresponding welding test ID (e.g., "`20250512_4`"), ensuring consistent organization and easy identification. Finally, the system is integrated with a cloud-based database, allowing remote access to all the collected data.

4.3 Automatic Parameter Extraction

To extract the process parameters from the collected images of the DCE1500 display, an automatic two-stage procedure was developed.

In the first stage, image processing is performed mainly by a YOLOv11 neural network trained to segment the display, isolating the relevant foreground while filtering out the background. Morphological operations, specifically a closing followed by an opening, are applied to clean the segmentation mask. This mask is then subjected to perspective correction in order to standardise the output, and finally, the region of interest (ROI) is reduced to only the table containing the process parameters.

In the second stage, optical character recognition (OCR) was necessary to extract the aforementioned parameters. Several OCR tools, including `pytesseract`, `EasyOCR`, and `Keras-OCR`, were tested but all proved ineffective. Consequently, a second YOLOv11 model was trained to recognise and extract the characters from the ROI. This OCR model was pre-trained using a publicly available dataset in Roboflow (Phil, 2023). Once the characters were identified, their values were extracted based on the known positions of each parameter within the table.

5 RESULTS

The external system sensorisation behaved as expected, even under the demanding conditions of the welding environment, which included sudden temperature variations, sparks, smoke, and electromagnetic noise. Despite such challenges, it was possible to capture data without interruptions or difficulties.

To explore the correlation between the monitored parameters and final weld quality and to generate a diverse dataset, several experiments were conducted under varying conditions. Using the Factory Twin, process variables such as weld current and duration were adjusted. In total, 46 different combinations of current and process duration were tested, resulting in approximately 200 experimental welds. During each experiment, both sensor data and process parameters were recorded.

With the recording data available, the performance of the automatic parameter extraction algorithm was evaluated in two stages: (1) initial segmentation of the display, and (2) character recognition.

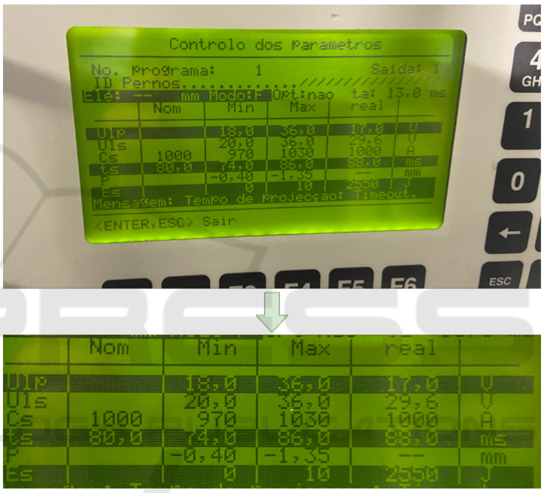

Figure 7: Example of the display segmentation.

For the first stage, 15% of the dataset was reserved as test data. The results were promising, with the model achieving a mean Average Precision at Intersection over Union (IoU) 0.50 to 0.95 (mAP50-95) of 99.8%. Figure 7 illustrates this step with an example showing both the input image and the resulting segmented ROI.

For the second stage of the algorithm, 10% of the dataset was used for evaluation, with each image containing approximately 70 characters. The results were less favourable, with a mAP50-95 of 67.7%. Nevertheless, the practical results were still acceptable, with most errors being related to the recognition of the minus ("-") character. Figures 8 and 9 show two examples of the character recognition algorithm's output.

Having now both sensor data and process control parameters available in a suitable format, a preliminary data analysis was conducted. Since the final weld quality classifications were not yet available, the focus of this analysis was to verify whether the vari-

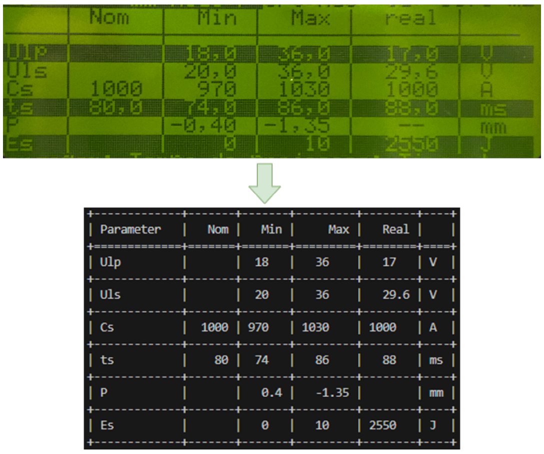

Parameter	Nom	Min	Max	Real	
Ulp		18	36	17	V
Uls		20	36	29.6	V
Cs	1000	970	1030	1000	A
ts	80	74	86	88	ms
P		0.4	-1.35		mm
Es		0	10	2550	J

Figure 8: Character recognition output from the OCR algorithm - Example 1.

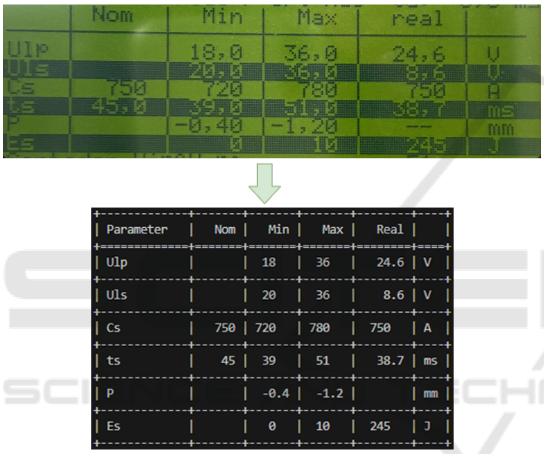

Parameter	Nom	Min	Max	Real	
Ulp		18	36	24.6	V
Uls		20	36	8.6	V
Cs	750	720	780	750	A
ts	45	39	51	38.7	ms
P		-0.4	-1.2		mm
Es		0	10	245	J

Figure 9: Character recognition output from the OCR algorithm - Example 2.

ables showed the expected behaviours. To that end, plots were generated using Python libraries such as `matplotlib.pyplot`, `pandas`, and `numpy`, illustrating how sensor readings varied over time.

Figures 10, 11, and 12 illustrate the plots generated from the collected data for one test iteration. As previously mentioned, the variables monitored during this preliminary analysis were selected based on findings from the literature (Table 1).

In Figure 10, it can be observed that during the lift and plunge moments of the welding process (see Figure 1b and 1c), indicated by a drop in the `DIST[mm]` value, which represents the distance between the welding gun and the welding surface, there is a corresponding spike in both CO concentration (`CO[ppm]`) and the welding plate temperature (`T_CHAPA_IR[C]`).

These variations are expected: the momentary increase in CO concentration likely indicates gas emissions caused by the welding arc, possibly due to the

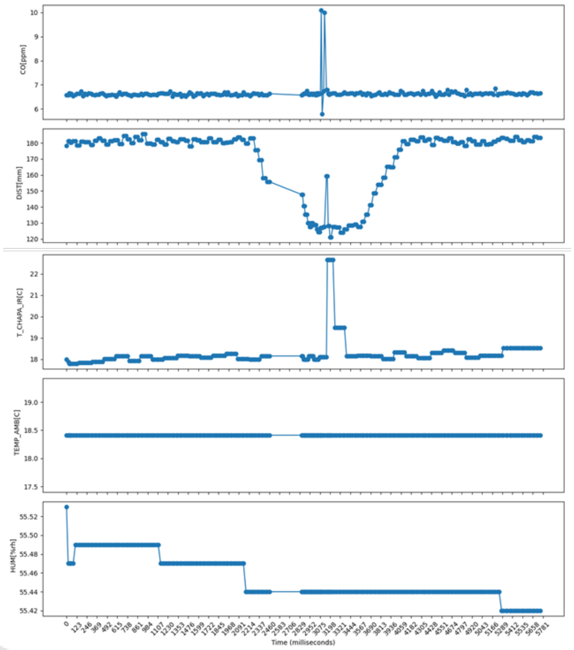

Figure 10: Variation of CO concentration, welding surface distance, welding surface temperature, ambient temperature, and ambient humidity, respectively, throughout the welding cycle.

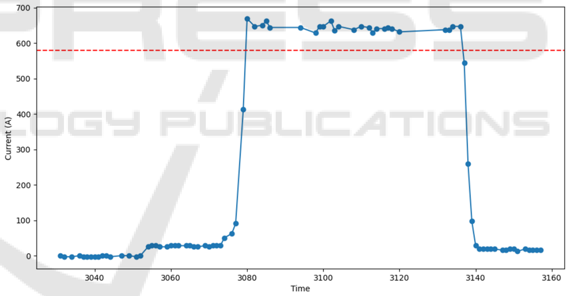

Figure 11: Approximation of the weld current near the peak during the welding cycle.

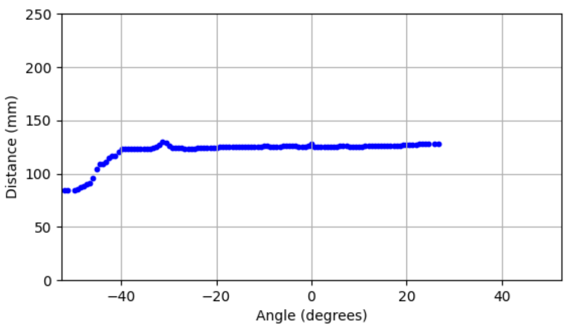

Figure 12: Visualization of point cloud data captured during the welding cycle.

combustion of surface materials. Similarly, the quick rise and drop in the welding plate temperature reflects the material's heating during the arc, followed by a quick cooling once the arc is extinguished.

The room ambient temperature (`TEMP_AMB[C]`) stays constant during the welding process, confirming that the rise in the welding plate temperature is a local effect and not due to a change in the overall environment. Humidity (`HUM[%]`) also shows very little variation, specifically around 0.1 percentage points, which is negligible considering the characteristics of the sensor.

The peak current plot in Figure 11 shows the same waveform shape as expected from the reference in Figure 4. The red line represents the nominal current value reported by the control unit during the weld. The close match between the measured and expected values shows that the sensor can accurately capture the welding current.

Finally, the point cloud visualisation in Figure 12 shows the data collected by the LiDAR sensor. As mentioned in Section 4, this sensor was mainly used to measure the inclination of the plate, which corresponds to the stud incidence angle. For most angles measured, the distance values remain nearly constant, which indicates that the welding plate is flat and parallel to the welding gun. From the conducted experiments, it was observed that when the plate was not parallel or not flat, the resulting welds were visibly of poor quality or even broken. Therefore, this suggests that plate inclination and surface flatness are relevant parameters for detecting and predicting poor quality welds.

Based on this example and the analysis of data from additional test iterations, it can be concluded that the collected sensor data exhibits the expected patterns. This confirms that the selected variables are suitable for characterizing the welding process. Furthermore, these results validate the sensor setup and establish a foundation for the development of future models to predict weld quality.

6 CONCLUSIONS AND FUTURE WORK

During automated SW processes, particularly in automotive assembly lines, low-quality welds can not only compromise the quality of the final product but also cause production delays due to the need for manual rework. Real-time weld quality prediction systems can help identify potential defects early in the assembly process, allowing operators to take corrective actions immediately and mitigate these issues.

This paper presents the first development stage of an AI-based system for real-time weld quality assessment in an automated SW process. It focuses on the study of the relevant variables that characterise the welding process and their correlation with final weld quality, as well as the welding setup sensorisation, and the development of a data acquisition system to build a dataset for future predictive model development. A Flask-based application was developed as part of the acquisition system to provide an interface for data collection. Additionally, an automatic character recognition algorithm was developed to extract welding parameters from images of the control unit display, as this data could not be extracted directly.

Through a series of welding experiments, testing with different variations of process parameters, an initial dataset of approximately 200 samples was generated. The implemented sensors performed well under the challenging welding conditions, and the automatic parameter extraction algorithm showed promising results. The preliminary data analysis confirmed the expected trends and variations in the recorded parameters.

Overall, these initial results show that the system was able to effectively capture data from the welding process, enabling the development of the predictive model. Future work will focus on improving the parameter extraction algorithm and performing weld quality classifications on the experimental samples to generate labelled data to train a supervised quality prediction model.

ACKNOWLEDGEMENTS

This work was financially supported by *PPS 14: Quality control predictive system for soldering* from *Agenda GreenAuto: Green Innovation for the Automotive Industry*, no. C644867037-00000013, investment project no. 54, from the Incentive System to Mobilising Agendas for Business Innovation, funded by the Recovery and Resilience Plan and by European Funds NextGeneration EU.

REFERENCES

Agenda GreenAuto (2021). Agenda greenauto: Green innovation for the automotive industry. https://www.agendagreenauto.pt/. Accessed: 2025-05-12.

Al-Sahib, N. K. A., Ameer, H. K. A., and Ibrahim, S. G. F. (2009). Monitoring and quality control of stud welding. *Al-Khwarizmi Engineering Journal*, 5(1):53–70.

Chambers, H. A. (2001). Principles and practices of stud welding. *Pci*, 46:46–59.

Klaric, S., Kladarić, I., and Kozak, D. (2010). The influence of the stud arc welding process parameters on the weld penetration. *BULETIN ŞTIINŢIFIC, Seria C / SCIENTIFIC BULLETIN, Series C*, XXIII(Fascicle: Mechanics, Tribology, Machine Manufacturing Technology).

Naddaf-Sh, S., Naddaf-Sh, M.-M., Dalton, M., Ramezani, S., Kashani, A. R., and Zargarzadeh, H. (2023). Application of machine learning in automotive stud weld defect classification. *IEEE Sensors Journal*, 23(20):25547–25556.

Phil (2023). Digits object detection dataset. https://universe.roboflow.com/phils-workspace/digits-coi4f/dataset/3. Accessed: 2025-07-25.

PT. Unggul Semesta. Dce control and energy source. https://www.unggulsemesta.com/brand/tucker/product/dce-control-and-energy-source/. Accessed: 2025-05-13.

Samardzic, I., Klaric, S., and Siewert, T. (2007). Analysis of welding parameter distribution in stud arc welding. Proceedings of the Conference: Welding and Materials, Dubrovnik, Croatia, 1, YU.

T. Lienert, T. Siewert, S. B. V. A. (2011). Stud arc welding. In *Welding Fundamentals and Processes*. ASM International.